High-Power Density Piezoelectric Energy Harvesting Using Radially Strained Ultrathin Trigonal Tellurium Nanowire Assembly

Tae Il Lee, Sangmin Lee, Eungkyu Lee, Sungwoo Sohn, Yean Lee, Sujeong Lee, Geondae Moon, Dohyang Kim, Youn Sang Kim, Jae Min Myoung, and Zhong Lin Wang**

Based upon the energy-conversion by a nanostructured material's piezoelectricity, the piezoelectric nanogenerator (NG) is a nanoscale power generator that transforms ambient mechanical energy into a useful form of electrical energy. Since the p-NG was introduced,[1] the wurtzite structure-based piezoelectric nanowires (NWs), ZnO NW,[2–6] GaN NW,[7] and CdS NW,[8] and the perovskite structure-based ferroelectric NWs, $NaNbO_3$ NW,[9] $BaTiO_3$ NW,[10] and $PbZr_xTi_{1-x}O_3$ NW,[11] have been considered as highly efficient piezoelectric components in the NG. The fundamental mechanism of NW-based NGs is related to the piezoelectric potential generated in the NWs when they are dynamically strained under an external force and the corresponding transient flow of electrons in an external load to balance the potential.

Thus far, many researchers have designed NGs so that they form the main piezoelectric strain in the longitudinal direction of the NWs, as the elongation of the NW is generally convenient in this direction as compared to the radial direction. Along the longitudinal direction, the NW has an asymmetric crystal structure constructed by the strong bonding between positive ions and negative ions.

Dr. S. Lee,[+] Prof. Z. L.Wang
Schools of Materials Science and Engineering
Georgia Institute of Technology
Atlanta, Georgia, 30332-0245,USA
E-mail: zhong.wang@mse.gatech.edu
Dr. T.I. Lee,[+] S.W. Sohn, S.J. Lee, Prof. J. M. Myoung, Prof. D.H. Kim
Department of Materials Science and Engineering
Yonsei University
Seoul, Korea
E-mail: jmmyoung@yonsei.ac.kr
E. Lee, Prof. Y.S. Kim
Advanced Institutes of Convergence Technology
864-1 Lui-ong, Yeongtong-gu, Suwon-si, Gyeonggi-do &
Program in Nano Science and Technology
Graduate School of Convergence Science and Technology
Seoul National University, Seoul, Korea
Y. Lee
Department of Mechanical Engineering
Georgia Institute of Technology
Atlanta, Georgia 30332-0245, USA
G. Moon
Department of Chemistry
University of California
Riverside, California, USA
[+] These authors equally contributed to this work.

DOI: 10.1002/adma.201300657

Unlike these conventional NWs, an ultrathin trigonal Te nanowire (t-Te NW) known as a single-component metallic bonding-based piezoelectric material[12] with a high work function[13] (4.95 eV) and a narrow bandgap energy[14] (0.35 eV) shows an asymmetric crystal structure in its radial direction. In a t-Te NW, Te atoms are covalently connected via an infinite helical turn at 120° along its longitudinal direction and all turns are bound to hexagonal bundles in its radial direction by weak van der Waals force.[15,16] Hence, we believe that a NG using NWs with an asymmetric crystal structure like the t-Te NW should be designed with the main piezoelectric strain in the radial direction. However, fundamental study of such a case may not exist

Furthermore, the t-Te NW has a strong potential to serve as a basis material for an ultrathin NG showing a high-volume power density because it is one of the narrowest NWs with a strain piezoelectric coefficient of 5.5×10^{-9} cm/V (d_{11}) that is the highest among all exiting piezoelectric NWs. From this point of view, the t-Te NW has sufficient value to be explored as a new class of piezoelectric material for future NGs.

To obtain a high power density NG, the NW should be laterally assembled in a form of monolayer on a substrate. The direct lateral growth[17] and physical sliding array[18] were introduced to get the lateral alignment in case of ZnO NWs, but these approaches are complicated in an industrial point of view and not suitable for the t-Te NW which has a different direction of main piezoelectric stain from its longitudinal direction. Therefore, another strategy have to be found to form a laterally aligned t-Te NW's monolayer with a crystallographically preferred orientation behaving as a single crystal.

Here, we theoretically and experimentally determined the direction of the main piezoelectric strain in t-Te NW having a radially asymmetric crystal structure and introduced a rapid chemical assembling route to form a uniaxially aligned ultrathin (<10 nm) t-Te NWs' monolayer with a crystallographically preferred orientation for a NG having a high power volume-density. Moreover, based upon a solution-processed high-yield mass-production protocol for t-Te NW,[19] our approach industrially has a significant meaning in the way to drive the t-Te NW to be an promising nanomaterial offering high performance for NG.

A schematic configuration of an ideally designed t-Te NW-based NG is shown in **Figure 1**a. As described here, the longitudinal directions of all of the t-Te NWs are adjusted so that they are parallel to the bending line of the NG, and t-Te NWs having a hexagonal shaped cross-section[20,21] are closely packed, facing

ADVANCED MATERIALS
www.advmat.de

www.MaterialsViews.com

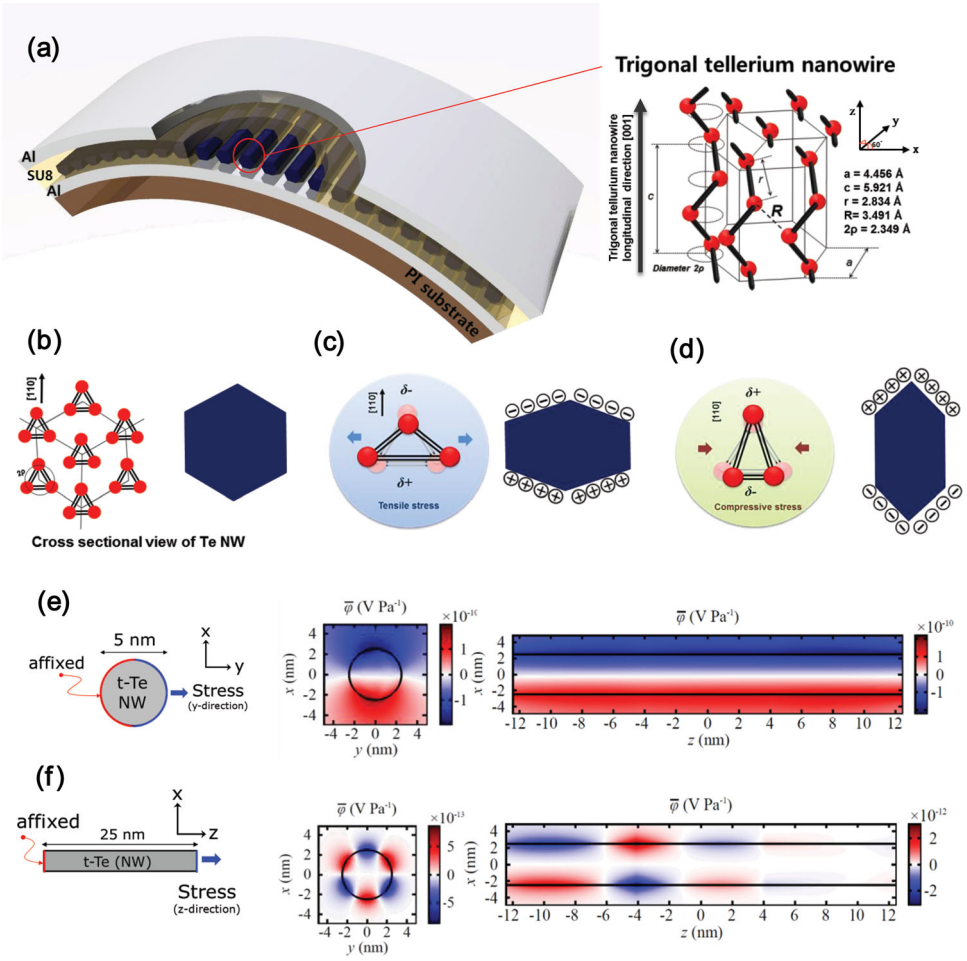

Figure 1. a) A bent NG consisting of well-aligned single crystalline t-Te NWs which are buried in a SU8 layer between aluminum electrodes on a PI substrate. b) A cross-sectional view of a t-Te NW. c) The dipole moment arises along the [$\bar{1}\bar{1}$0] direction under tensile stress. (d) The [110] directional dipole moment is generate under compressive stress d. (e) The piezoelectric potential distribution in the case of tensile stress in the radial direction y. (f) The piezoelectric potential distribution in the case of tensile stress in the longitudinal direction z.

each other at their hexagonal sides in the monolayer. This facial packing between t-Te NWs gives the monolayer a {110} plane preferred crystallographic orientation on a flat substrate.

Based on the crystal structure of the t-Te NW illustrated in the schematic diagram at the bottom of Figure 1a, the piezoelectric potential is generated only by the strain in the {001} plane;[22] thus, it is predicted that adjustments of the longitudinal direction of the t-Te NW to the bending line as well as the facial packing are required at the same time to generate piezoelectric power from the t-Te NWs. The mechanism for the generation of the piezoelectric potential from the ideally designed NG given these two conditions is explained qualitatively as follows.

Without the strain, the hexagonal cross-section of the t-Te NW and its two-dimensional hexagonal-lattice structure with equilateral triangles results from the projection of the helical turns of Te atoms onto the {001} plane are illustrated in Figure 1b. When tensile stress is applied along the radial direction of the t-Te NW on the (110) plane, the shape of the cross-section changes to a horizontally stretched hexagon and the equilateral triangle contorts into an obtuse-angle isosceles triangle, resulting in a displacement of the positive Te ions and displacement of the electronic negative charge center against the Te cores, leading to downward piezoelectric polarization, as shown in Figure 1c. On the other hand, in case of compressive stress is applied, the shape of the cross-section becomes a vertically expanded hexagon and the equilateral triangle contorts into an acute-angle isosceles triangle and upward piezoelectric polarization is generated, as shown in Figure 1d.

Theoretically, to verify the effectiveness of the design of the NG in Figure 1a and the above suggested mechanism, we calculated the piezoelectric potential generated from a t-Te NW. For this calculation, there were several assumptions (see the Supporting Information). The piezoelectric potential of the t-Te NW induced by stress was calculated using a finite element method with COMSOL Multiphysics®. Two principle directions of a tensile stress to be applied to a t-Te NW laid on a substrate were considered, the radial direction (along the y-axis) and the longitudinal direction (along the z-axis), as shown in Figures 1e and f, respectively. In the case of tensile stress along the y-axis, the piezoelectric potential was generated along the x-axis and the potential was uniformly distributed over the entire surface of the t-Te NW, as exhibited in Figure 1e. The mechanism for the generation of the

DOI: 10.1002/adma.201300657

piezoelectric potential was such that strain in the y-direction led to displacements of the positive Te ions and the electronic negative charge with respect to the Te cores, as the crystallographic symmetry of the t-Te NW is only broken by the strain in the x or y direction. On the other hand, in the case of tensile stress along the z-axis, the piezoelectric potential was locally generated but perfectly offset in all directions, as exhibited in Figure 1f. Thus, the overall piezoelectric voltage cannot be theoretically generated in this case. The perceived reason behind this result was that no displacement would be created between the positive and negative charges in the t-Te NW because its crystallographic symmetry is always maintained under strain along the c-axis.

The t-Te NWs in the monolayer must be uniaxially aligned and have a crystallographically preferred orientation on a substrate, as the piezoelectricity of t-Te NW strongly depends on its crystal orientation, as mentioned above. Therefore, to impart the preferred orientation to the monolayer, we adopted a fast-spreading method.[23] A real-time video clip to demonstrate this process and a camera image of the t-Te NW monolayer floating on water are included (see the Video Supporting Information and Figure S1 in the Supporting Information).

The quality of the directional alignment of the t-Te NWs on the monolayer was determined using a cross-polarized optical microscope (CPOM) (see the Figure S2 in the Supporting Information). To confirm the quality of the alignment of the t-Te NWs, the monolayer was observed using a transmitting electron microscope (TEM) (**Figure 2**a). Uniform t-Te NWs having a high aspect ratio exceeding 1000:1 were well-aligned in the horizontal direction and were assembled into a continuous monolayer film.

Besides the directional alignment of the t-Te NWs, the preferred orientation on a substrate is an essential condition to generate piezoelectric power from a NG. From the x-ray diffraction (XRD) analysis shown in Figure 2b, the crystallographic orientation of the monolayer on a glass substrate was revealed to be on the {110} plane. Because the thickness of the monolayer was less than 10 nm, the background peaks from the glass substrate are larger than those of the monolayer. However, there was a clear peak identified by {110} plane indexing.

To obtain clearer evidence of the preferred orientation, the selective area electron diffraction (SAED) pattern was determined. This result is exhibited in Figure 2c. The center pole represents the [110] direction and the nearest two poles are defined as (001) and $(\bar{1}10)$, while the pole of (001) represents the direction of the c-axis in t-Te NWs. The relationships between the SAED pattern and the crystal orientations were confirmed from the calculation of the reciprocal lattice of the t-Te and the aligning feature of the t-Te NWs in the white dotted circle, which indicates the electron beam spot, as shown in Figure 2d. The result showing that nearly 20 well-aligned t-Te NWs have the same SAED pattern with a [110] center pole affirms the {110} preferred orientation of the monolayer, which was formed using a fast spreading method and was transferred onto a substrate.

Lastly, for the final confirmation of the {110} preferred orientation, the orientation of the crystal lattice of a single t-Te NW included in the monolayer was directly observed by means of high-resolution TEM. This result is shown in Figures 2e and f. The diameter of the t-Te NW was about 5 nm, and the helical turn repeated by three Te atoms was clearly observed from the magnification of an area, as indicated by the white dotted square in Figure 2e. To determine the crystallographic orientation of the t-Te NW, the real lattice structure of the t-Te NW shown in Figure 2f was moved into a reciprocal lattice space using a live fast Fourier transformation (FFT) tool. The result is displayed in Figure 2g. Using a reciprocal lattice calculation of the FFT pattern, it was found that the center pole is defined by [110] and that the nearest two poles are represented by (001) and $(\bar{1}10)$. This result precisely matches the result from the SAED pattern in Figure 2c. Consequently, based upon all evidence presented in Figures 2, the {110} preferred crystallographic orientation of the monolayer was confirmed.

Under the bending shown in the insets of **Figures 3**a and b, tensile stress is applied to all of the t-Te NWs in a direction

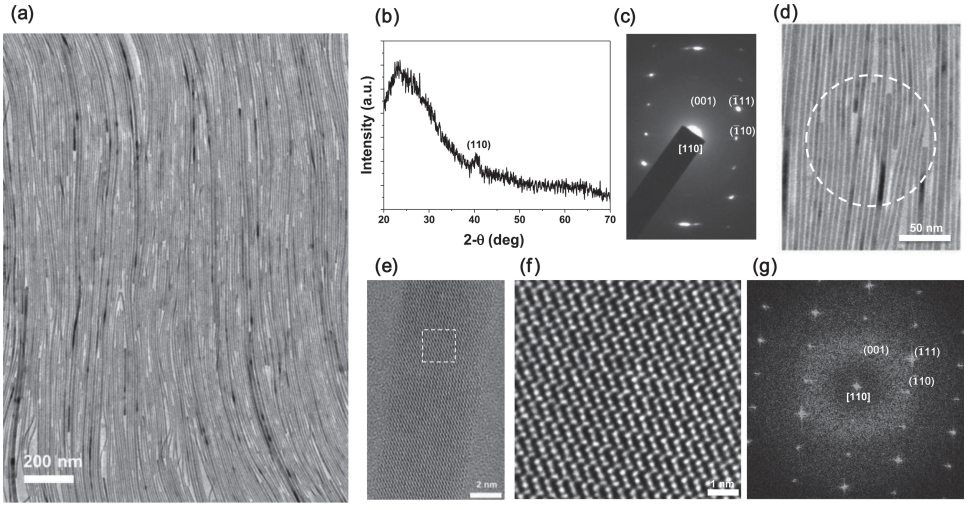

Figure 2. (a) The top-view TEM image of the monolayer. (b) From the XRD analysis of the monolayer on a glass substrate, only a peak-indexed as (110) was determined. (c) SAED pattern of the t-Te NW film. (d) The white dotted circle indicates the selected area. (e) High-resolution TEM analysis of a t-Te NW. The (110) orientation of the NW on the TEM grid definitely is confirmed from the magnification image (f) and the FFT image (g) of white dotted square.

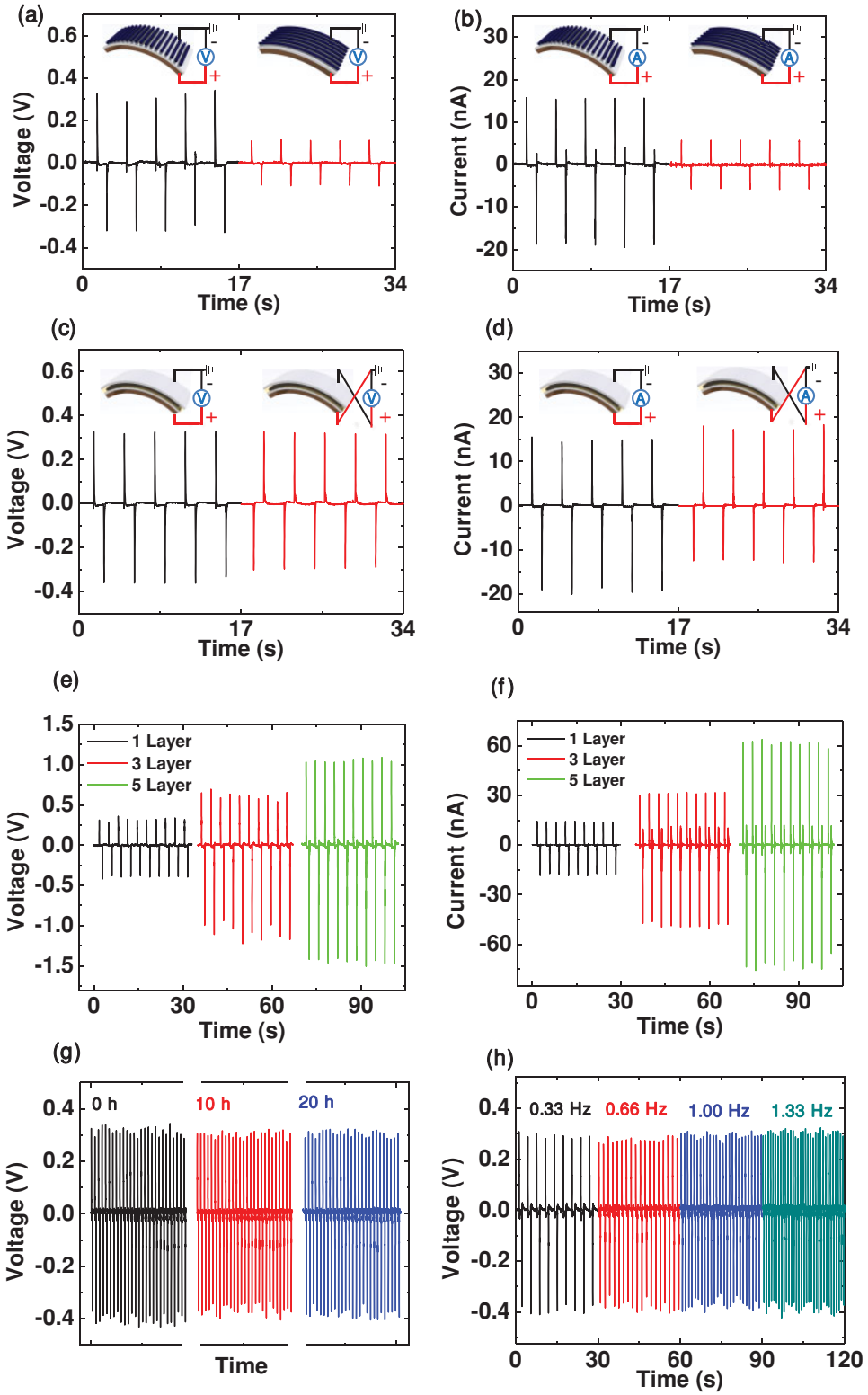

Figure 3. According to the aligned direction of the t-Te NWs, the output voltage of NGs (a) and the output current of NGs (b) under tensile stress as induced by bending are shown. (c) The output voltage of NG with forward and reverse connections. (d) The output current of NG with forward and reverse connections. (e) The output voltage with 1,3, and 5 layers. (f) The output current with 1,3, and 5 layers. Stability depending on the (g) time and (h) frequency using a sample of a single layer.

Adv. Mater. **2013**,
DOI: 10.1002/adma.201300657

perpendicular to the bending line. The output voltage and current in the NG consisting of the t-Te NWs aligned parallel to the bending line were three times higher than those in the NG consisting of the t-Te NWs aligned perpendicularly. The fact that the performance of the output voltage and current of the NGs strongly depended on the bending line with respect to the c-axis of the t-Te NW was precisely in accordance with the predictions by the theoretical calculations.

Strictly speaking, the generation of a piezoelectric voltage is theoretically impossible when the t-Te NWs are aligned perpendicularly to the bending line, as described in the calculation part, but the output voltage (~0.1 V) and current (~10 nA) were experimentally measured in this case. This unusual electrical output came from the imperfect alignment of the t-Te NWs, as clearly observed from many stains in the CPOM images in Figure S2. Consequently, it was thought that all electrical outputs shown in Figures 3a and b were only generated from the t-Te NWs receiving tensile stress in the radial direction, as with the mechanism demonstrated in our calculation.

The power density of our NG shown in Figures 3a and b was estimated to be 9 mW/cm^3 under the 0.13% strain and 2.2%s^{-1} straining rate. Considering the 400-fold thicker SU8 layer than the monolayer of the t-Te NWs, we supposed that the power density would show more of an increase because there was a margin to reduce the capacitance of the NG by nearly 400 times. In the capacitively coupled NG, its capacitive reactance is proportional to its thickness; therefore, the voltage drop that forms between the dielectric layer decreases as its thickness decreases. Therefore, based upon the intrinsically high piezoelectric constant of the t-Te NW, the power density may be enhanced.

As shown in Figures 3c and d, we confirmed that the open-circuit voltage and short-circuit current were completely reversed when the polarity was switched. In addition, we measured the electrical performance with an increase in the number of stacked t-Te NW layers under the same condition. As the number of layers increases from 1 to 3 and then to 5, the output voltage increases from 0.3 to 0.6 and then to 1.0 V, and the output current increases from 15 to 30 and then to 60 nA, respectively, as shown in Figures 3e and f. Because the same bending force simultaneously affects the stacked t-Te NW layers and their corresponding piezoelectric potential values are summed, an enhancement of the piezoelectric potential can lead to an increase in both the output voltage and the output current. These results show the evidence of the piezoelectricity of the t-Te NW as well as the possibility of a scale-up to increase the output performance. Further, we confirmed that the polarity of the electrical output was reversed when the type of stress, from tensile to compressive, was changed (see Figure S3 in the Supporting Information). Thus, these results clearly show that the source of the output power in the NG is the piezoelectricity of the t-Te NW.

In addition, the output voltage of t-Te NW-based NG was not deteriorated after 20 hours of operation, as well as not significantly affected when the driving frequency was increased from 0.33 to 1.33 Hz, as shown in Figures 3g and h. Given that the excellent stability of our device enables energy harvesting from irregular excitation in our living environment, these advantages provide great potential for use in practical applications.

In summary, a ultrathin (<10 nm) t-Te NW was introduced as a new class of piezoelectric nanomaterial having a radially asymmetric crystal structure for a NG. Considered the crystal structure of t-Te NW, an ideal design for the t-Te NW-based NG was suggested. To verify the effectiveness of the qualitative design, a theoretical calculation of two possible stretching modes of t-Te NWs in a bending operation was executed using a finite element method. As a result, the fact that strain only in the radial direction of the t-Te NW activates its piezoelectricity was confirmed. With a monolayer of well-aligned t-Te NWs produced using a fast-spreading method, a NG having a power density of 9 mW/cm^3 was fabricated. The NG presented different performance levels according to the aligned direction of the t-Te NWs with respect to the bending line, in agreement with the theoretical prediction. From the perspective of introducing the t-Te NW as a new class of piezoelectric material, the long-term stability and bending frequency stability of the t-Te NW-based NG were measured, and its excellent stability in these situations was experimentally confirmed. Consequently, we derived a design route in which the direction of the main piezoelectric strain in the t-Te NW-based NG has to be adjusted to the direction of the asymmetry in its crystal structure. As the thickness of the dielectric layer in the NG is optimized so as to reflect the superior piezoelectricity of the t-Te NW on the output power, its significantly advanced performance compared to that of a conventional NG is expected. Also, we believe that this study of the t-Te NW can be expanded to the various ultrathin chalcogenide NWs, as the t-Te NW has been used as a template to obtain various telluride compounds showing useful properties, converting various types of ambient energy into electrical energy using properties such as piezoelectricity, thermoelectricity and pyroelectricity.

Supporting Information

Supporting Information is available from the Wiley Online Library or from the author.

Acknowledgements

This research was supported by WCU (World Class University) program (R32-20031), the Basic Research Program (2011-0018113) through the National Research Foundation of Korea funded by the Ministry of Education, Science and Technology, U.S. Department of Energy, Office of Basic Energy Sciences (DE-FG02-07ER46394), NSF (0946418), MANA, National Institute For Materials, Japan.

Received: February 8, 2013
Published online:

[1] Z. L. Wang, J. Song, *Science* **2006**, *312*, 242–246.
[2] X. Wang, J. Song, J. Liu, Z. L. Wang, *Science* **2007**, *316*, 102–105.
[3] S. Xu, B. J. Hansen, Z. L. Wang, *Nat. Nanotechnol.* **2010**, *5*, 366–373.
[4] Y. Qin, X. Wang, Z. L. Wang, *Nature* **2008**, *451*, 809–813.
[5] S. Lee, J. I. Hong, C. Xu, M. Lee, D. Kim, L. Lin, W. Hwang, Z. L. Wang, *Adv. Mater.* **2012**, *24*, 4398.
[6] S. Lee, S.-H. Bae, L. Lin, Y. Yang, C. Park, S. W. Kim, S. N. Cha, H. Kim, Y. J. Park, Z. L. Wang, *Adv. Funct. Mater.* **2012**, DOI10.1002/adfm.201202867.

[7] C. Huang, J. Song, W. Lee, Y. Ding, Z. Gao, Y. Hao, L. Chen, Z. L. Wang, *J. Am. Chem. Soc.* **2010**, *132*, 4766–4771.
[8] Y. Lin, J. Song, Y. Ding, S. Lu, Z. L. Wang, *Appl. Phys. Lett.* **2008**, *92*, 022105.
[9] J.H. Jung, M. Lee, J. Hong, Y. Ding, C. L. Chen, Z. L. Wang, *ACS Nano* **2011**, *12*, 10041–10046.
[10] Z. Wang, J. Hu, A. P. Suryavanshi, K. Yum, M. Yu, *Nano Lett.* **2007**, *7*, 2966–2969.
[11] S. Xu, B. J. Hansen, Z. L. Wang, *Nat. Commun.* **2010**, *1*, 93.
[12] D. Royer, E. Dieulesaint, *J. Appl. Phys.* **1979**, *50*, 4042.
[13] David R. Lide, *Handbook of Chemistry and Physics*, 88th Ed., CRC press **2008**, 12–114.
[14] A. A. Kudryavstev, *The Chemistry and Technology of Selenium and Tellurium*, Collet's Ltd., London **1974**.
[15] W. C. Cooper, *Tellurium*, Van Nostrand Reinhold Co., New York **1971**
[16] L. I. Berger, *Semiconductor Materials*, CRC Press, Boca Raton, FL **1997**, 86–88.
[17] S. Xu, Y. Qin, C. Xu, Y. Wei, R. Yang, Z. L. Wang, *Nat. Nanotechnol.* **2010**, *5*, 366–373.
[18] G. Zhu, R. Yang, S. Wang, Z. L. Wang, *Nano Lett.* **2010**, *10*, 3151–3155.
[19] Y. Zhu, X. Hu, W. Wang, *Nanotechnology* **2006**, *17*, 645–650.
[20] N. Furuta, Y. Ohasi, H. Itinose, Y. Igarashi, *Jpn. J. Appl.Phys.* **1975**, *14*, 929.
[21] N. Furuta, H. Itinose, N. Maruyama, Y. Ohasi, *Jpn. J. Appl. Phys.* **1972**, *11*, 1113.
[22] G. Arlt, P. Quadflieg, *Phys. Stat. Sol* **1969**, *32*, 687–689.
[23] G. Moon, T. I. Lee, B. Kim, G. Chae, J. Kim, S. Kim, J. Myoung, U. Jeong, *ACS Nano* **2011**, *5*, 8600–8612.

Adv. Mater. **2013**,
DOI: 10.1002/adma.201300657